Journal of
Proteomics & Bioinformatics

Yonezawa et al., J Proteomics Bioinform 2014, 7:11
DOI: 10.4172/jpb.1000337

Research Article Open Access

Comparative Proteomics and Network Analysis Identify PKC Epsilon Underlying Long-Chain Fatty Acid Signaling

Tomo Yonezawa[1,2,3]*, Riho Kurata[1,3,4], Atsushi Tajima[1], Xiaofeng Cui[5], Hiroki Maruta[3], Hirofumi Nakaoka[1], Keiichi Nakajima[6] and Hidetoshi Inoko[1]

[1]*Division of Basic Medicine Science and Molecular Medicine, School of Medicine, Tokai University, Bohseidai, Ishehara, Kanagawa 259-1193, Japan*
[2]*Department of Pharmacology and Therapeutic Innovation, Nagasaki University, Graduate School of Biomedical sciences, 1-14 Bunkyo-machi, Nagasaki 852-8531, Japan*
[3]*Research Institute for Biomedical Sciences, Tokyo University of Science, 2669 Yamazaki, Noda, Chiba 278-0022, Japan*
[4]*Japan Society for the Promotion Science, Japan*
[5]*School of Chemistry, Chemical Engineering and Life Science, Wuhan University of Technology, 122 Luoshi Road, Wuhan, Hubei 430070, China*
[6]*NARO Hokkaido Agricultural Research Center, Hitsujigaoka 1, Toyohira, Sapporo 062-8555, Japan*

Abstract

Long-chain fatty acid possesses myriad roles in the biological function of the cells, not only as an energy substrate but also as substrates for cell membrane synthesis and as precursors for intracellular signaling molecules. However, little is known about the biological pathways that are stimulated by long-chain fatty acid. In order to identify the pathway of long-chain fatty acid, we performed 2-dimensional gel electrophoresis in the cells treated with or without oleate, and then analyzed 648 protein spots using PDQuest software and narrowed down 22 significant changing spots by statistical criterion. We also tried to determine these spots by MALDI-QIT-TOF-MS and SWISS-PROT database query. We identified 11 proteins and predicted the biological network using available data sets from protein-protein interaction database. This prediction indicated that several protein kinase Cs (PKCs) underlie long-chain fatty acid signaling. Indeed, oleate stimulated predicted PKC pathways. In expression array, oleate significantly up-regulated only PKC epsilon, but not other PKCs, in transcriptional levels. Collectively, our proteomics and network analysis implicates that PKC epsilon pathway plays an important role in long-chain fatty acid signaling.

Keywords: Long-chain fatty acid; Protein kinase C epsilon (PKCε); 2 Dimensional gel electrophoresis; MALDI-QIT-TOF-MS/MS; Network analysis

Abbreviations: LCFAs: Long-Chain Fatty Acids; PPARs: Peroxisomal Proliferators-Activated Receptors; SREBPs: Sterol Response Element Binding Proteins; GPCRs: G Protein-Coupled Receptors; MEK: Mitogenic Extracellular Kinase; ERK: Extracellular Signal-Regulated Kinase; PI3K: Phosphatidylinositol 3-Kinase; 2-DE: Two-Dimensional Electrophoresis; MALDI-QIT-TOF-MS: Matrix Assisted Laser Desorption/Ionization Quadrupole Ion Trap-Time-of Flight Mass Spectrometry; PKC: Protein Kinase C; DMEM: Dulbecco's Modified Eagle Medium; DTT: Dithiothreitol; CAN: Acetonitrile; TFA: Trifluoroacetic Acid; bMEC: Bovine Mammary Epithelial Cell; DHB: 2, 5-Dihydroxybenzoic Acid; CID: Collision-Induced Dissociation; PVDF: Polyvinylidene Difluoride; TBST: Tris-Buffered Saline Containing 0.1% Tween-20; cRNA: Complementary RNA; FDR: False Discovery Rate; DAVID: Database for Annotation, Visualization and Integrated Discovery; UCP: Uncoupling Protein

Introduction

Long-chain fatty acids (LCFAs) are an important source of energy and possess myriad effects on various tissues [1], while, LCFAs play a pivotal role in the pathogenesis of insulin resistance and type 2 diabetes [2-4]. Patients with insulin resistance and type 2 diabetes possess symptom of lipid metabolism disorder, especially high blood LCFAs level [5]. Classically, two transcriptional factors are thought to control LCFA signaling. One is peroxisomal proliferators-activated receptors (PPARs) belonging to a family within the lipid-activated receptor superfamily are activated by LCFAs [6,7]. Three PPARs have been identified in mammals, PPAR alpha, beta/delta and gamma [6,7]. These are thought to have a critical role in energy and lipid metabolism. Unsaturated LCFAs (n-9, n-6 or n-3) can act as ligands to activate all three PPARs [7]. The other is sterol response element binding proteins (SREBPs), a family of transcriptional factor regulating genes involved in the synthesis of cholesterols and fatty acids [8]. Recently, GPR40, one of the G protein-coupled receptors (GPCRs), was reported to bind to LCFAs [9-11]. We and other groups demonstrated that functioning G protein-coupled receptor for LCFAs, GPR40 induces cell-proliferation via mitogenic extracellular kinase (MEK) 1/2/extracellular signal-regulated kinase (ERK) 1/2 and phosphatidylinositol 3-kinase (PI3K)/Akt pathways in normal and malignant mammary epithelial cells [12,13]. However, signaling pathways of LCFAs have still not been completely elucidated.

In this study, we set out to identify differential expression profiles of protein and mRNA by treatment of LCFA. We performed the combination of two-dimensional electrophoresis (2-DE) and matrix assisted laser desorption/ionization quadrupole ion trap-time-of flight mass spectrometry (MALDI-QIT-TOF-MS) and expression array. We identified and analyzed 648 protein spots and finally narrowed down 22 spots. Among 22 spots, we identified 11 proteins by MALDI-QIT-TOF-MS and established biological network using their data sets of protein-protein interaction (PPI). We predicted several protein kinases C (PKC) underlies LCFA signaling and indeed confirmed that LCFA can activate them. Further we obtained gene expression profiles in the

***Corresponding author:** Tomo Yonezawa, Division of Basic Medicine Science and Molecular Medicine, School of Medicine, Tokai University, Bohseidai, Ishehara, Kanagawa 259-1193, Japan, Tel : +81-4-7121-4105; Fax: +81-4-7121-4104; E-mail: yonet2301@yahoo.co.jp;yonet@rs.tus.ac.jp; yonet@nagasaki-u.ac.jp

Received September 10, 2014; **Accepted** October 09, 2014; **Published** October 14, 2014

Citation: Yonezawa T, Kurata R, Tajima A, Cui X, Maruta H, et al. (2014) Comparative Proteomics and Network Analysis Identify PKC Epsilon Underlying Long-Chain Fatty Acid Signaling. J Proteomics Bioinform 7: 340-346. doi:10.4172/jpb.1000337

Copyright: © 2014 Yonezawa T, et al. This is an open-access article distributed under the terms of the Creative Commons Attribution License, which permits unrestricted use, distribution, and reproduction in any medium, provided the original author and source are credited

cells and then, our result of expression profile indicates LCFA activates only PKC epsilon in transcriptional level. We concluded that PKC epsilon underlies LCFA signaling and suggest that it plays an important role for lipid metabolism and response.

Materials and Methods

Materials

Dulbecco's Modified Eagle Medium (DMEM) and Trizol reagent were obtained from Invitrogen Corp. (Carlsbad, CA, USA). A 12.5% e-Pagel gel was obtained from Atto Co. (Tokyo, Japan). Precision Plus Protein Kaleidoscope Standards were obtained from Bio-Rad Laboratories, Inc. (Hercules, CA, USA). Sodium oleate, dithiothreitol (DTT), ammonium bicarbonate, iodoacetamide, octyl beta-D-glucopyranoside, acetonitrile (ACN) and trifluoroacetic acid (TFA) were purchased from Sigma-Aldrich (St. Louis, MO, USA). Zip Tip C18 was obtained from Millipore (Billerica, MA, USA). Skim milk powder was purchased from Difco Laboratories (Detroit, MI, USA). Anti-human PKC epsilon (sc-214) was obtained from Santa Cruz Biotechnology, Inc. (Santa Cruz, CA, USA). PKC Isoform Antibody Sampler Kit #9960, anti-14-3-3 zeta/delta (#9639) and anti-cyclophilin A (#2175) were obtained from Cell Signaling Technology Inc. (Beverly, MA, USA). Anti-cytokeratin 8 (ab2531), anti-cytokeratin 19 (ab84632), anti-annexin II (ab2242) and anti-ATP5B (ab14730) Anti-transgelin 2 was obtained from Protein Tech Group, Inc. (Chicago, IL, USA). Secondary HRP-conjugated anti-rabbit IgG, glutathione-sepharose, Immobiline DryStrip pH 3-11NL and IPG buffer 3-11NL were purchased from GE Healthcare Bioscience, Co. (Piscataway, NJ, USA). Bovine Gene Expression Microarray (4x44K V2:023647), Low Input Quick Amp Labeling kit and wash buffer were obtained from Agilent Technologies Inc. (Santa Clara, CA, USA).

Cell cultures

Bovine mammary epithelial cell (bMEC) was isolated and cloned by Nakajima et al. [14]. The cells were seeded at 1×10^4 cells/cm^2 in a collagen coated 6-well plate (Corning, NY,) and grown in DMEM supplemented with 10% FCS, 2 mM glutamine, 100 U/ml penicillin, and 100 µg/ml streptomycin under 5% CO_2 and air at 37°C until confluency. The cells were treated with serum-deprivation overnight and subsequently with 400 µM oleate conjugated to 0.5% BSA or BSA alone for 24 h. We then carried out the experiments according to following procedures.

2-D gel electrophoresis

The cells were lysed by sonication at 4°C in cell lysis buffer (8.5 M urea, 40 mM Tris-HCl, pH 8.0, 10 % w/v SDS, 20% v/v Triton X-100 and 2% w/v DTT) containing protease inhibitor cocktail. After that, protein concentration was determined by 2-D Quant kit and thus an equal amount of each sample was used for 2-DE. 2-D gel electrophoresis was performed with the Ettan IPGphor II and Ettan DALTsix equipment from GE Healthcare. For the first dimension, samples in 450 µl rehydration buffer (6M urea, 2M thiourea, 0.2% w/v DTT, 2% IPG buffer 3-11 nonlinear, 0.1M acetic acid, 0.1% w/v orange G and 20% triton X-100) were loaded in the IPGphor strip holder. 24 cm immobiline DryStrip (pH 3-11 nonlinear) was placed in a holder and overlaid with DryStrip coverfluid. Strips were hydrated under 50 V for 24 h and focused afterward on the IPGphor II IEFsystem for a total of 80 kVh at 20°C. After electrophoresis, each strip was incubated with 7.5 ml of equilibration buffer (6M urea, 100 mM Tris-HCl, pH 8.0, 30 % w/v glycerol, 2% w/v SDS, 0.5% w/v DTT and 0.002% bromophenol blue) by rocking for 20 min. For the second dimension, the strips were placed on top of 10-20% gradient polyacrylamide gel containing SDS. Then SDS-PAGE was performed using Ettan DALT six electrophoresis system. After second dimension, the gels were fixed with 50% methanol and 10% acetic acid for 30 min, subsequently with 10% methanol and 7% acetic acid for 30 min and washed with distilled water for 30 min. After that, the gels were stained with SYPRO Ruby overnight in dark, washed with 10% methanol and 7% acetic acid for 30 min and washed with distilled water for 10 min.

Scanning and image analysis

After staining, images of the gels were directly scanned by Fluoro Phore Star 3000 (Anatech) and analyzed by PDQuest (Bio-Rad Hercules, CA). Briefly, the background between each gel was normalized and its noise was deleted. Experiments were replicated to ensure consistency. Identification and normalization of the number of protein spots was done. After that, we matched all of the spots among all of the gels. After all, we identified 648 spots and narrowed down 22 spots using statistical criteria (not less than 3-fold change and t-test; $P<0.01$).

Spot picking and in-gel digestion

To identify proteins significantly changed by oleate, each protein spot position was determined, excised robotically and transferred to tube using Fluoro Phore Star 3000. Each piece of gel was destained with 25 mM ammonium bicarbonate in 50% acetonitrile and washed with 25 mM ammonium bicarbonate, and subjected to reduction by 10 mM dithiothreitol and alkylation by 55 mM iodoacetamide. Subsequently, the piece of gel was digested with Trypsin Gold (Mass spec grade, Promega) overnight at 37°C. The digested peptides were extracted from the gel piece by 50% acetonitrile containing 5% trifluoroacetic acid. The extracts were evaporated in vacuum centrifuge to remove organic solvent and concentrated. Finally the extracts were desalted, concentrated using reverse-phase C18 Zip Tip (Millipore) and then eluted directly onto MALDI target plate by 50% acetonitrile containing 2, 5-dihydroxybenzoic acid (DHB) matrices.

MALDI-QIT-TOF-MS analysis

MALDI-QIT-TOF mass spectrometer (AXIMA resonance) equipped with a nitrogen laser (337 nm, 3 ns pulse with) (Shimazu, Kyoto, Japan) was used. The ion trap chamber was supplied with two separate and independent gases; He gas with continuous flow was used for collisional cooling, and pulsed Ar gas was used for imposing collision-induced fragmentation. The pressure in the ionization chamber was maintained at less than 6×10^{-6} Torr. Precursor and fragment ions obtained by collision-induced dissociation (CID) were ejected from the ion trap and analyzed by a reflectron TOF detector operated in positive ion mode. The mass spectra were assembled 200 to 3000 accumulations of the profile obtained by laser shots using a laser power of 30-60 arbitrary units. Stronger laser power (around 100) increased sensitivity of MS and provided fragment ions used as the precursor ion for sequential MS/MS analysis. Experimental calibration of MS spectra was performed using angiotensin II ($[M + H]^+$, m/z 1046.5) and ACTH ($[M + H]^+$, m/z 2465.2) on MALDI target plate. We performed MASCOT searches (http://www.matrixscience.com/search_form_select.html) using SWISS-PROT sequence database. One missed cleavage and partial oxidation of methionine were allowed. Peptide mass tolerance in MS searches was set to less than 0.2 Da. We were sure to exclude the spectra of trypsin and human keratin peptides.

Network analysis

In order to explore biological pathways using identified proteins (red circle) and their interacting proteins (pink circle), we sought to identify their interacting proteins in a large human protein interaction database (BioGrid) (http://thebiogrid.org/) [15]. We constructed a network graph, in which the edges represented a physical interaction between two proteins. CytoScape software (http://www.cytoscape.org/) was used to visualize the network [16].

Western blot analysis

The translocation of each PKC from the cytosolic fraction to the membrane fraction in cells was used to assess the relative amounts of activated and membrane-bound PKC epsilon, as described previously [17]. Active translocation was identified as either an increase in the amount of PKC in the membrane fraction or a decrease in the cytosolic fraction. The cells were washed with cold PBS, scraped into homogenization buffer, passed through a syringe needle (27-gauge), and spun at 100,000x g for 30 min at 4°C. The supernatant was collected as the cytosolic fraction. The pellet was then extracted using homogenization buffer with 1% Triton X-100, and the extracted buffer was collected as the membrane fraction. Cytosolic fraction was used for other molecules. Equal amounts of protein samples were electrophoresed on an E-PAGE 48 8% gel before being transferred to polyvinylidene difluoride (PVDF) membranes using an iBlot™ Gel Transfer Device. The membranes were blocked with 5% skim milk/Tris-buffered saline containing 0.1% Tween-20 (TBST) at room temperature for 1 h. The samples were then incubated with rabbit anti-human PKC epsilon for 1 h at room temperature. Membranes were washed three times with TBST, incubated for 1 h at room temperature with HRP-conjugated anti-rabbit IgG, washed six times with TBST, and visualized using ECL+. Experiments were replicated three times to ensure consistency.

Statistical analysis

In experiments of Western blot analysis, values are expressed as the mean ± S.E.M. of at least triplicate samples in each experimental group; experiments were replicated to ensure consistency. Statistical significance was determined using t-test. Values were considered to be statistically significant if their *P* value was less than 0.05.

Microarray analysis

The principal methods for microarray were described previously [18]. In Brief, Gene Expression microarray for cow (G2519F; 4 x 44K) and all of the reagents for microarray were obtained from Agilent Technologies Inc. (Santa Clara, CA, USA). Quadruplicate total RNA were extracted from cells treated with or without oleate using Trizol reagent as described [13] and its integrity was assessed using an Agilent Bioanalyzer 2100. Each aliquots of total RNA was reverse transcribed into complementary DNA and subsequently transcribed into complementary RNA (cRNA) using the Low Input Quick Linear Amp Labeling Kit. The quality of each cRNA was confirmed by total yield and specificity calculated using NanoDrop ND-1000 spectrophotometer (Thermo Fisher Scientific, MA, USA). Labeled cRNAs were used for hybridization. Slides for microarray were incubated at 65°C for 17 h in microarray hybridization chambers. After hybridization, slides were washed according to the protocol suggested by Agilent. Images for each array were scanned with an Agilent DNA microarray scanner (model G2505C) and saved as TIFF format. For data normalization, 75 percentile normalization using a per chip 75 percentile of all measurements were performed by GeneSpring GX software (Agilent Technologies Inc., Santa Clara, CA, USA). P value and fold changes (more than 1.5-fold) between each comparison for each gene were calculated. False discovery rate (FDR) (q values) were calculated by Gene Spring software according to Benjamini and Hochberg's method. Differentially expressed genes were analyzed using Database for Annotation, Visualization and Integrated Discovery (DAVID) to predict biological pathways [19, 20].

Results

Profile of protein expression induced by LCFA

To obtain profile changed by treatment of LCFA, we performed 2-DE in cloned bovine mammary epithelial cells treated with or without oleat. The representative pattern of 2-DE was shown in Figure 1. We could assign 648 protein spots among each image of triplicate samples and also ensure reproducibility of both the pattern and all of them (data not shown). Finally, we narrowed down 22 spots using statistical criteria (not less than 3-fold change and t-test; P<0.01).

Determination of protein spots

To determine proteins changed by treatment of LCFA, we picked up significant 22 spots, performed in-gel digestion and subsequently performed MS/MS analysis by MALDI-QIT-TOF-MS. We searched

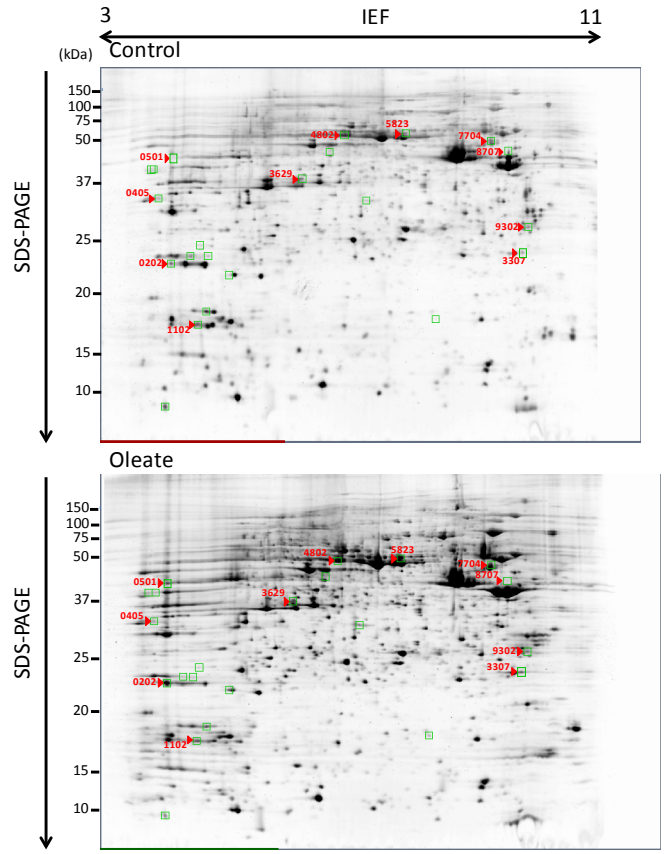

Figure 1: Protein profiling of bovine mammary epithelial cells treated with LCFA. The cells were treated with serum-deprivation overnight and subsequently with 400 μM oleate (lower panel) conjugated to 0.5% BSA or BSA alone (lower panel) for 24 h. Representative data of 2-DE according to the procedures shown in Materials and Methods. Green squares indicate significant changed protein spot assigned by PDQuest software. Red arrowhead and number indicate protein spot number identified by MS/MS ion search.

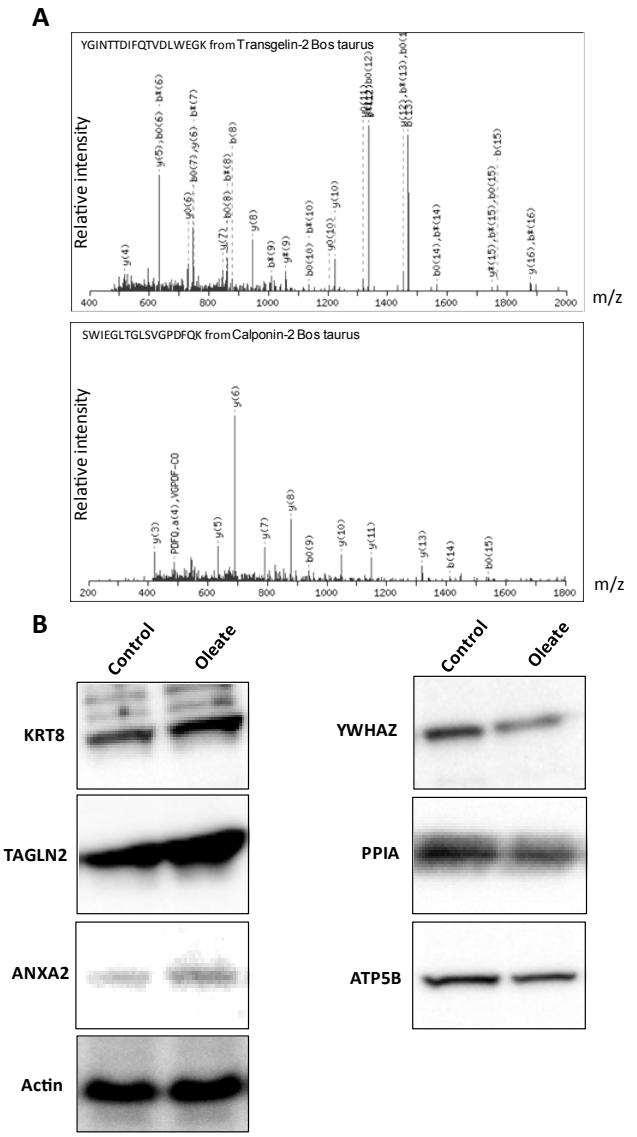

Figure 2: Identification of proteins changed by LCFA. (A) Representative data of MS/MS spectra are shown. Upper panel indicates the spectrum of Bos taurus Transgelin-2 peptides. Lower panel indicates that of Bos taurus Calponin-2. (B) The cells were treated with serum-deprivation overnight and subsequently with 400 μM oleate (lower panel) conjugated to 0.5% BSA or BSA alone (lower panel) for 24 h. After that, cell lysates were analyzed by western bloting using specific antibodies against KRT8, TAGLN2, ANXA2, YWHAZ, PPIA, ATP5B and actin. The Figure shows data from a representative experiment.

identical proteins using MASCOT database. Among them, we succeeded in determining 11 proteins (Figure 2A and Table 1). All of them were identical to bovine homologue (Table 1). AXNA2, KRT8 and TAGLN2 were significantly increased, while KRT7, ATP5B, KRT19, YWHAZ, HNRNPA1, PPIA, ALB and CNN2 were significantly reduced. To confirm whether or not identified proteins are changed by treatment of LCFA, we also performed western blotting. Most of them were identical with the results of 2-DE (Figure 2B).

Prediction of LCFA-induced biological pathway using PPI data sets

To identify biological pathway underlying LCFA signaling, we tried to construct a network based on available data sets from PPI database. We could predict tight network using data sets of identified 11 proteins although data set of CNN2 could not connected that of any other proteins (Figure 3A). Depicted pathway indicates several PKCs such as PKC alpha, delta, iota, zeta and mu, underlie LCFA signaling (Figure 3A).

PKC epsilon underlies LCFA signaling

To validate predicted several PKCs pathway actually underlies LCFA signaling, we examined whether LCFA induces the translocation of each PKCs or not. Our result of western blotting indicated that LCFA significantly induced the translocation of several PKC such as PKC alpha, delta, epsilon and mu (Figure 3A red arrow head and B) although the expression of PKC zeta was low. The amount of membrane-bound PKC alpha, delta, zeta, epsilon and PKD relative to those of cytosolic were around 3.0-, 2.2-, 1.2-, 2.0- and 2.4-fold, respectively (Figure 3B). We also obtained a profile of gene expression in same condition. 299 genes were significantly changed by treatment of LCFA (data not shown). 230 genes were induced, while 69 were reduced (Supplemental data 1). Using DAVID algorithm, we could significantly predict PPAR signaling (P value<0.01) and primary immunodeficiency (P value<0.05) (supplementary data 1 and 2). Among identified proteins, PRKCE, KRT17 and FCGRT are significantly induced up to 2-fold, 3.7-fold and 2-fold, respectively (Figure 2A blue arrow head and supplementary data 1). KRT17 was also significantly induced up to around 8-fold by LCFA treatment in protein level (Figure 3B). Taken together, we concluded that PKC epsilon induction in both mRNA and protein level is an important for LCFA signaling.

Discussion

We for the first time demonstrated that several PKCs underlie LCFA signaling using combination with 2-DE, differential expression analysis, MALDI-QIT-TOF-MS and pathway analysis based on PPI. It's important that activated PKCs translocate from cytosolic into cellular membrane fractions including golgi, endoplasmic reticulum, mitochondria and nucleus [21]. Indeed, we demonstrated that the translocation of predicted PKCs are enhanced by LCFA. Besides that, PKC epsilon is only activated by LCFA in both protein and transcriptional levels. Our pathway prediction clearly indicates that LCFA induces Akt and ERK1/2 pathway via probably GPR40 [22]. This is coincidence with previous reports [12,22]. However, we also previously reported that LCFA induces up-regulation of uncoupling protein (UCP) 2 mRNA [23]. Although our prediction indicates that LCFA affects UCP2, our gene expression array could not detect any change of UCP2 mRNA. However, the probe of UCP2 on microarray platform used in this study is not efficient to detect because it is located in an intermediate region between DNAJB13 and UCP2, which is much closer to 3' untranslated region of DNAJB13 and so far from UCP2 promoter region (probe number is A_73_115660, it's located in chr.15:052961966-052962025). That's because the probe could not detect UCP2 mRNA expression.

We also identified Annexin A2, mitochondrial ATP synthase subunit beta, 14-3-3 protein zeta/delta, Transgelin-2, Heterogeneous nuclear ribonucleoprotein A1, Peptidyl-prolyl cis-trans isomerase A, Calponin-2 and several cytokeratines in LCFA signaling. Annexin A2 is involved in nociception in brain [24,25]. PKC epsilon is also well known to be involved in nociception [21]. These suggest that Annexin A2 may be regulated by PKC epsilon. Indeed, LCFA induces up-regulation of Annexin A2 through PPAR alpha and the translocation of Annexin A2 as well as PKC epsilon [26,27]. Coincidence with them, our result

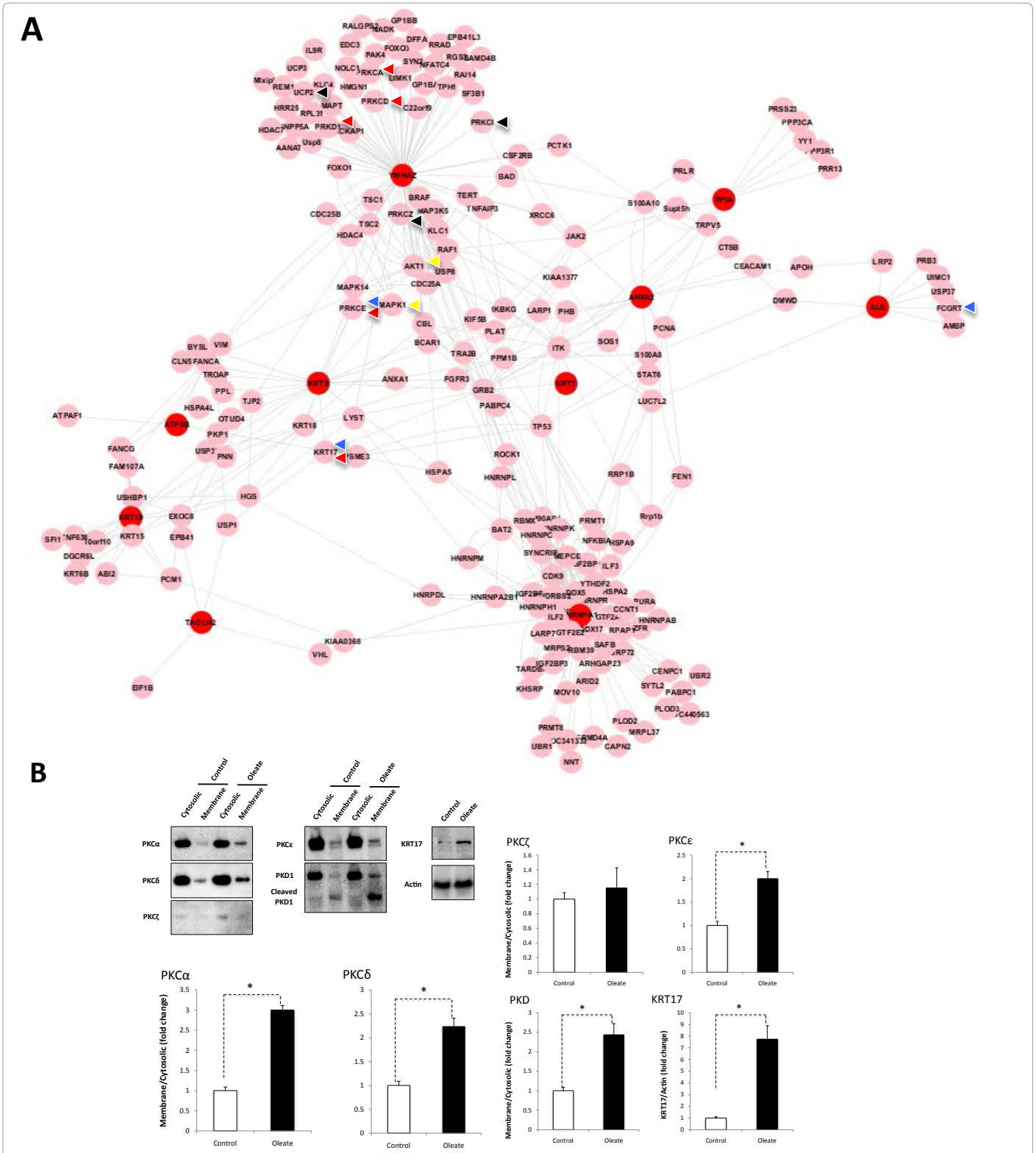

Figure 3: Predicted PKCs are actually activated by LCFA. (A) Prediction of biological pathway based on data sets of identified proteins obtained from public protein-protein interaction database, BioGrid. Red circles indicate identified protein, while pink circles indicate molecules, which can bind identified protein. The edges indicate physical interaction between two molecules. Red arrowhead indicates PKC activations, which is confirmed by this study. Black one indicates PKC activations, which is not confirmed by this study, otherwise that UCP2, which is reported to up-regulation by our previous study in transcriptional level, could not observe any change in microarray in this study. Yellow one indicates molecules, which are reported to activation by LCFA in our previous study. Blue one indicates molecules, which is significantly induced by LCFA in microarray in this study. (B) Cell lysates were separated as cytosolic and membrane fractions, and analyzed by western blotting using antibodies against each PKCs. The Figure shows data from a representative experiment. The rates of translocation are expressed as fold changes relative to control cells (membrane protein density normalized against those of the cytosolic fraction). The amounts of KRT17 are expressed as fold changes relative to control cells. The data are expressed as means ± SEM (n=3). Asterisk indicates significantly different ($P<0.05$, t-test).

Spot No. Protein name	Sequence coverage	Determined peptide sequence	Theoretical value	
			p/	Mr (kDa)
3629 Annexin A2 Bos taurus up	5%	16 AYTNFDAERDALNIETAIK	6.92	38.9
	4%	20 GVDEVTIVNILTNR		
4802 Keratin, type II cytoskeletal 7 Bos taurus down	2%	54 VDTLNDEINFLR	5.79	51.6
5823 Keratin, type II cytoskeletal 8 Bos taurus up	2%	32 LEGLTDEINFYR	5.6	51.6
7704 ATP synthase subunit beta, mitochondrial Bos taurus down	2%	65 FTQAGSEVSALLGR	5.15	56.3
	3%	30 FLSQPFQVAEVFTGHLGK		
	3%	50 DQEGQDVLLFIDNIFR		
8707 Keratin, type I cytoskeletal 19 Bos taurus down	4%	27 NLLEGQDAYFNDLSLAK	4.92	43.9
9302 14-3-3 protein zeta/delta Bos taurus down	8%	19 LGLALNFSVFYYEILNSPEK	4.73	27.9
	7%	13 GIVDQSQQAYQEAFEISK		
0202 Transgelin-2 Bos taurus up	9%	24 YGINTTDIFQTVDLWEGK	8.39	22.6
	9%	57 QYDADLEQILIQWITTQCR		
	7%	54 DDGLFSGDPNWFPK		
	7%	13 QMEQISQFLQAAER		
0405 Heterogeneous nuclear ribonucleoprotein A1 Bos taurus down	4%	8 GFAFVTFDDHDSVDK	9.27	34.3
	5%	9 LFIGGLSFETTDESLR		
1102 Peptidyl-prolyl cis-trans isomerase A Bos taurus down	9%	9 SIYGEKFDDENFILK	8.34	18.1
	10%	18 VNPTVFFDIAVDGEPLGR		
0501 Serum albumin Bos taurus down	2%	22 DAFLGSFLYEYSR	5.82	71.2
3307 Calponin-2 Bos taurus down	5%	49 SWIEGLTGLSVGPDFQK	7.55	33.8
	5%	18 SMQNWHQLENLSNFIK		

Table 1: Proteins changed by Oleate and Identified by 2-Dimentional Electrophoresis.

indicates that LCFA induces an increase of Annexin A2 proteins. Besides that, in insulinoma cell lines, INS-1, LCFA induces down-regulation of mitochondrial ATP synthase subunit beta proteins [28], which plays an important role for mitochondrial ATP synthesis utilizing an electrochemical gradient of proton across the inner membrane during oxidative phosphorylation [28]. We also observed the similar result in this study. Several studies indicate that 14-3-3 zeta/delta protein directly binds PKC epsilon and modulates its activity [29,30]. Both PKC epsilon and 14-3-3 zeta/delta play an important role for cytokinesis including actin polymerization [30]. Using unique method combined with *in vitro* kinase reaction, ion exchange chromatography, 2-DE and MS analysis, Dammeier et al. [31] demonstrated that transgelin-2 (a.k.a. smooth muscle protein 22-alpha) is a novel substrate of PKC and its ability to bind actin filament is regulated by PKC. Moreover, calponin, which is an another actin-binding protein, are regulated and stabilized through its phosphorylation by PKC epsilon and their function is an important in contraction and differentiation of smooth muscle cells [32,33]. Taken together, we implicates that our identified proteins are involved in PKC epsilon signaling and that our prediction network reflects LCFA-induced PKC epsilon signaling.

Novak et al. [34] identified that keratin, type II cytoskeletal 8 is down-regulated in liver in rat fed with high unsaturated LCFA diet through gestation and lactation. We also observed that LCFA induces down-regulation of the same keratin in mammary epithelial cells. These reports and our result suggest that PKC epsilon underlies LCFA signaling. Simple epithelial keratins, such as KRT7, KRT8, K18-K20, are expressed in single-layered simple epithelia and are also thought that they have some functions not only in cellular structure, but also in some cellular responses [35]. Indeed, KRT8-deficient mice were shown to have liver hemorrhage with embryonic lethality in C57Black/6 background [36]. Besides that, in FVB/n background, the mice were shown to have colitis and hepatitis [37]. KRT18 can bind 14-3-3 zeta/delta and control hepatocyte mitotic progression [38]. In mice lacking KRT19, overexpression of KRT18 and KRT20 to compensate its function [39,40], suggesting KRT19 has an ability to bind 14-3-3 zeta protein as well as KRT18. These cytokeratin networks may be involved in LCFA-induced PKC epsilon signaling.

Our prediction based on both profiles of protein and mRNA indicates that KRT17 plays an important role as well as PKC epsilon. With respect to engagement of Keratin in protein synthesis, Kim et al. [41] demonstrated that epidermal keratins play a critical role in promoting protein synthesis, cell size and growth through association of KRT17 with 14-3-3 proteins. Besides that, this mechanism is involved in Akt/mTOR pathway [41]. Our prediction included Akt/mTOR pathway and indicated that the nodes of KRT8, KRT17, KRT18, Akt, TSC1, TSC2, 14-3-3 zeta/delta and PKC epsilon are so close and formed as tight network. In our preliminary data, LCFA stimulates cellular protein contents and synthesis in mammary epithelial cells possibly for milk proteins such as casein and lactoglobulin. Probably, LCFA induces Akt/mTOR pathway because this pathway is an essential for protein synthesis. Our predicted network including keratin and PKC epsilon may be involved in Akt/mTOR pathway.

In conclusion, using a combination of 2-DE, MALDI-QIT-TOF-MS and prediction of biological pathway based on PPI data sets, we identified 11 proteins induced by LCFA and predicted some PKC pathways underlie LCFA signaling. In fact, we confirmed the changes of identified proteins and the activation of predicted PKCs. Further microarray analysis revealed that PKC epsilon and KRT17 are up-regulated in both transcriptional and protein levels. We concluded that PKC epsilon underlies LCFA signaling and suggest that it may play an important role for protein synthesis and lipid metabolism.

Acknowledgement

This work was supported by Tokai University School of Medicine Research Aid and a Grant-Aid for Young Scientists (B) from Japan Society for Promotion of Science (JSPS- 22710194). We thank Education and Research Support Center (Tokai University School of Medicine) for their technical assistance.

References

1. Chawla A, Repa JJ, Evans RM, Mangelsdorf DJ (2001) Nuclear receptors and lipid physiology: opening the X-files. Science 294: 1866-1870.

2. Boden G, Chen X, Ruiz J, White JV, Rossetti L (1994) Mechanisms of fatty acid-induced inhibition of glucose uptake. J Clin Invest 93: 2438-2446.

3. Kelley DE, Mokan M, Simoneau JA, Mandarino LJ (1993) Interaction between glucose and free fatty acid metabolism in human skeletal muscle. J Clin Invest 92: 91-98.

4. Shulman GI (2000) Cellular mechanisms of insulin resistance. J Clin Invest 106: 171-176.

5. Boden G (1997) Role of fatty acids in the pathogenesis of insulin resistance and NIDDM. Diabetes 46: 3-10.

6. Green S (1995) PPAR: a mediator of peroxisome proliferator action. Mutat Res 333: 101-109.

7. Forman BM, Chen J, Evans RM (1997) Hypolipidemic drugs, polyunsaturated fatty acids, and eicosanoids are ligands for peroxisome proliferator-activated receptors alpha and delta. Proc Natl Acad Sci USA 94: 4312-4317.

8. Brown MS, Goldstein JL (1997) The SREBP pathway: regulation of cholesterol metabolism by proteolysis of a membrane-bound transcription factor. Cell 89: 331-340.

9. Briscoe CP, Tadayyon M, Andrews JL, Benson WG, Chambers JK, et al. (2003) The orphan G protein-coupled receptor GPR40 is activated by medium and long chain fatty acids. J Biol Chem 278: 11303-11311.

10. Itoh Y, Kawamata Y, Harada M, Kobayashi M, Fujii R, et al. (2003) Free fatty acids regulate insulin secretion from pancreatic beta cells through GPR40. Nature 422: 173-176.

11. Kotarsky K, Nilsson NE, Flodgren E, Owman C, Olde B (2003) A human cell surface receptor activated by free fatty acids and thiazolidinedione drugs. Biochem Biophys Res Commun 301: 406-410.

12. Hardy S, St-Onge GG, Joly E, Langelier Y, Prentki M (2005) Oleate promotes the proliferation of breast cancer cells via the G protein-coupled receptor GPR40. J Biol Chem 280: 13285-13291.

13. Yonezawa T, Katoh K, Obara Y (2004) Existence of GPR40 functioning in a human breast cancer cell line, MCF-7. Biochem Biophys Res Commun 314: 805-809.

14. Nakajima K, Nakamura M, Gao XD, Kozakai T (2008) Possible involvement of prolactin in the synthesis of lactoferrin in bovine mammary epithelial cells. Biosci Biotechnol Biochem 72: 1103-1106.

15. Stark C, Breitkreutz BJ, Chatr-Aryamontri A, Boucher L, Oughtred R, et al. (2011) The BioGRID Interaction Database: 2011 update. Nucleic Acids Res 39: D698-D704.

16. Smoot ME, Ono K, Ruscheinski J, Wang PL, Ideker T (2011) Cytoscape 2.8: new features for data integration and network visualization. Bioinformatics 27: 431-432.

17. Brandman R, Disatnik MH, Churchill E, Mochly-Rosen D (2007) Peptides derived from the C2 domain of protein kinase C epsilon (epsilon PKC) modulate epsilon PKC activity and identify potential protein-protein interaction surfaces. J Biol Chem 282: 4113-4123.

18. Kurata R, Tajima A, Yonezawa T, Inoko H (2013) TRIM39R, but not TRIM39B, regulates type I interferon response. Biochem Biophys Res Commun 436: 90-95.

19. Huang da W, Sherman BT, Lempicki RA (2009) Systematic and integrative analysis of large gene lists using DAVID bioinformatics resources. Nat Protoc 4: 44-57.

20. Huang da W, Sherman BT, Lempicki RA (2009) Bioinformatics enrichment tools: paths toward the comprehensive functional analysis of large gene lists. Nucleic Acids Res 37: 1-13.

21. Yonezawa T, Kurata R, Kimura M, Inoko H (2009) PKC delta and epsilon in drug targeting and therapeutics. Recent Pat DNA Gene Seq 3: 96-101.

22. Yonezawa T, Haga S, Kobayashi Y, Katoh K, Obara Y (2008) Unsaturated fatty acids promote proliferation via ERK1/2 and Akt pathway in bovine mammary epithelial cells. Biochem Biophys Res Commun 367: 729-735.

23. Yonezawa T, Sanosaka M, Haga S, Kobayashi Y, Katoh K, et al. (2008) Regulation of uncoupling protein 2 expression by long-chain fatty acids and hormones in bovine mammary epithelial cells. Biochem Biophys Res Commun 375: 280-285.

24. Ayoub SS, Yazid S, Flower RJ (2008) Increased susceptibility of annexin-A1 null mice to nociceptive pain is indicative of a spinal antinociceptive action of annexin-A1. Br J Pharmacol 154: 1135-1142.

25. Foulkes T, Nassar MA, Lane T, Matthews EA, Baker MD, et al. (2006) Deletion of annexin 2 light chain p11 in nociceptors causes deficits in somatosensory coding and pain behavior. J Neurosci 26: 10499-10507.

26. Zhao H, Hardy RW (2004) Long-chain saturated fatty acids induce annexin II translocation to detergent-resistant membranes. Biochem J 381: 463-469.

27. Cherkaoui-Malki M, Meyer K, Cao WQ, Latruffe N, Yeldandi AV, et al. (2001) Identification of novel peroxisome proliferator-activated receptor alpha (PPARalpha) target genes in mouse liver using cDNA microarray analysis. Gene Expr 9: 291-304.

28. Köhnke R, Mei J, Park M, York DA, Erlanson-Albertsson C (2007) Fatty acids and glucose in high concentration down-regulates ATP synthase beta-subunit protein expression in INS-1 cells. Nutr Neurosci 10: 273-278.

29. Dai JG, Murakami K (2003) Constitutively and autonomously active protein kinase C associated with 14-3-3 zeta in the rodent brain. J Neurochem 84: 23-34.

30. Saurin AT, Durgan J, Cameron AJ, Faisal A, Marber MS, et al. (2008) The regulated assembly of a PKCepsilon complex controls the completion of cytokinesis. Nat Cell Biol 10: 891-901.

31. Dammeier S, Lovric J, Eulitz M, Kolch W, Mushinski JF, et al. (2000) Identification of the smooth muscle-specific protein, sm22, as a novel protein kinase C substrate using two-dimensional gel electrophoresis and mass spectrometry. Electrophoresis 21: 2443-2453.

32. Li L, Zhang Y, Zhou C (2012) Phosphorylation of h1 calponin by PKC epsilon may contribute to facilitate the contraction of uterine myometrium in mice during pregnancy and labor. Reprod Biol Endocrinol 10: 37.

33. Leinweber B, Parissenti AM, Gallant C, Gangopadhyay SS, Kirwan-Rhude A, et al. (2000) Regulation of protein kinase C by the cytoskeletal protein calponin. J Biol Chem 275: 40329-40336.

34. Novak EM, Lee EK, Innis SM, Keller BO (2009) Identification of novel protein targets regulated by maternal dietary fatty acid composition in neonatal rat liver. J Proteomics 73: 41-49.

35. Omary MB, Ku NO, Strnad P, Hanada S (2009) Toward unraveling the complexity of simple epithelial keratins in human disease. J Clin Invest 119: 1794-1805.

36. Baribault H, Price J, Miyai K, Oshima RG (1993) Mid-gestational lethality in mice lacking keratin 8. Genes Dev 7: 1191-1202.

37. Baribault H, Penner J, Iozzo RV, Wilson-Heiner M (1994) Colorectal hyperplasia and inflammation in keratin 8-deficient FVB/N mice. Genes Dev 8: 2964-2973.

38. Ku NO, Michie S, Resurreccion EZ, Broome RL, Omary MB (2002) Keratin binding to 14-3-3 proteins modulates keratin filaments and hepatocyte mitotic progression. Proc Natl Acad Sci USA 99: 4373-4378.

39. Tao GZ, Toivola DM, Zhong B, Michie SA, Resurreccion EZ, et al. (2003) Keratin-8 null mice have different gallbladder and liver susceptibility to lithogenic diet-induced injury. J Cell Sci 116: 4629-4638.

40. Stone MR, O'Neill A, Lovering RM, Strong J, Resneck WG, et al. (2007) Absence of keratin 19 in mice causes skeletal myopathy with mitochondrial and sarcolemmal reorganization. J Cell Sci 120: 3999-4008.

41. Kim S, Wong P, Coulombe PA (2006) A keratin cytoskeletal protein regulates protein synthesis and epithelial cell growth. Nature 441: 362-365.